

# Circular geodesics in the generalized q-metric

Shokoufe Faraji\*

*University of Bremen, Center of Applied Space Technology and Microgravity (ZARM), 28359 Germany*

In this paper, Weyl's procedure is used to investigate an alternative generalization of the q-metric that describes a deformed compact object in the presence of an external distribution of matter via exercising quadrupole moments. This work aims to examine quadrupole parameters' impact by studying the circular geodesic on the equatorial plane.

## I. INTRODUCTION

Finding exact and approximate solutions in general relativity describing the physical source is always of high interest. There exists quite a large number of the solutions of the Einstein field equations in the literature (for a review, see for example [1]). However, when this question is considered a deviation from the spherical symmetry, finding the answer is challenging.

On the other hand, within the general theory of relativity, Birkoff's theorem states that Schwarzschild space-time is the unique static solution of the asymptotically flat vacuum Einstein field equation with a regular event horizon. However, by considering a static mass distribution with a quadrupole moment, characterizing the deviation from spherical symmetry, this theorem will no longer be valid. Therefore it is possible to find the various vacuum solutions with mass and different quadrupole parameters.

In this paper, we mainly focus on two exterior solutions. The first class contains the asymptotically flat solutions. In this respect, the first static and axially symmetric solutions with arbitrary quadrupole moment are described by Weyl in 1917 [2]. Then Erez and Rosen discovered static solutions with arbitrary quadrupole in prolate spheroidal coordinates in 1959 [3]. Later Zipoy [4], and Voorhees [5] found a transformation that generates the simplest solution with quadrupole. This metric possesses interesting physical aspects with strange topologies, and for exact spherical symmetry reduces to the Schwarzschild metric. This metric is known as  $\gamma$ -metric or  $\sigma$ -metric, and later on, with representing it in terms of a new parameter is known as q-metric [6].

The above procedure; however, leads to having Minkowski space as the limiting case. In fact, this requirement of the asymptotic flatness assumption is equivalent to restricting isolated cases in the space. While this is natural to restrict ourselves, in the first place, to isolated compact objects, the question as to how the external distribution of mass may distort them might be of some interest. In this perspective, the second class of solution describes non-asymptotically flat space-time, which is obtained by assuming the existence of a static and axially symmetric external distribution of matter.

This space-time is a local solution of the Einstein field equation by its construction [7]. In 1965, Doroshkevich and his colleagues considered an external gravitational field up to a quadrupole in the Schwarzschild space-time. They also showed that by adding quadrupole correction to the Schwarzschild space-time, the horizon remains regular [8]. However, a detailed analysis of the distorted Schwarzschild space-time's global properties was introduced in 1982 by Geroch & Hartle [9]. Later the explicit form of this metric was presented in [10].

Both cases are of the high-interest field of study, from the mathematics and physics perspective and discussed extensively in the literature in many respects—for example, the first case [11–19], among many others.

In this paper, we generalize the static q-metric by considering a distribution of external matter by exercising quadrupoles. Thus, the result is not asymptotically flat by its construction. Mathematically, it is possible to find various vacuum solutions with mass and different quadrupole parameters. Nevertheless, differences appear only at the higher multipoles. This means that all the solutions can describe the exterior gravitational field of distorted mass distribution up to the quadrupole moment because they satisfy all the conditions necessary to describe the exterior gravitational field of realistic compact objects. One reason to choose this metric to work on as the first step is, the mathematical structure of the q-metric is straightforward, which facilitates its study and can be handled analytically. For instance, this metric would be the first option when searching for interior solutions considering matching conditions' mathematical complexity. So, the q-metric is the best candidate for this task after the Schwarzschild solution itself. From the physics perspective, this solution is similar to the q-metric solution with an additional external gravitational field, similar to the addition of a magnetic environment to the black hole solution. [20–23]. We expect to explore the rotation version in future works.

Several physical properties of the q-metric have been investigated in the literature, for instance [24–37] and references therein.

There are a number of motives to consider this generalization, aside from what is stated above about the simplicity of q-metric to be treated analytically. In the relativistic astrophysical study, it is assumed that astrophysical compact objects are described by the Schwarzschild or Kerr space-times. However, besides these relevant solutions, others can imitate a black hole's properties, such

---

\* shokoufe.faraji@zarm.uni-bremen.de

as the electromagnetic signature [38]. It is also possible that some astrophysical observations may not be fitted within the general theory of relativity by using the Schwarzschild or Kerr metric [39, 40]. It is also possible to measure the deviation from a Kerr black hole in cases of extreme mass ratio inspiral (EMRI). In this respect, this work aims at investigating how different backgrounds may describe an astrophysical phenomenon with departure from spherical geometry.

Second, in astrophysics, people attempt to determine the observable predictions of strong-field images of accretion flows in many ways. In this respect, this approach may provide an opportunity to take quadrupole moments as the additional physical degrees of freedom to the central compact object and its surroundings. This can facilitate searching for the link between observational phenomena and the compact object's properties which is not isolated. For example, the geometric configuration of an accretion disk located around this space-time depends explicitly on the value of both quadrupole parameters in a way that it is always possible to distinguish between a distorted Schwarzschild black hole and a distorted, deformed compact object. As another example, the Universe's accelerated expansion and the hypotheses of so-called dark matter and dark energy have led to the development of alternative gravity theories. It is expected by applying this model to relativistic cosmology; one may find potential possibilities that are linked to the parameters of the system.

Besides, there is no doubt of the fundamental importance of gravitational waves in physics, where the experimental evidence finally supported the purely theoretical research in this area. In fact, this metric can apply to the study of gravitational waves generated by a slightly non-isolated and self-gravitating axisymmetric distribution of mass. In fact, Ryan showed [41] that we can extract the multipole moments of the central body from the gravitational wave signal. Thus, any non-Kerr multipole moments should be encoded in the waves [42–44]. One can particularly apply this metric in the colliding gravitational waves where asymptotic flatness is not a requirement. As another example, the gravitational field of a very large plate of thin matter, where its gravity mainly focuses at a finite distance, and therefore it stops behaving well asymptotically [45].

As the next step of this work, one can add rotation also into this setup to be capable of describing more realistic scenarios. However, it has been shown [46] that, for example, the possible resonant oscillations of the thick accretion disk can be observed even if the source of radiation is steady and perfectly axisymmetric.

In this work, also we explore circular geodesics in the equatorial plane in this background in Section IV. There are studies on geodesics in both mentioned cases, for example [47–57] among many others.

Indeed, the properties of congruencies of circular and quasi-circular orbits in a static and axisymmetric background seems vital to comprehend accretion processes in

the vicinity of compact objects. In particular, the radial and vertical epicyclic frequencies are the most important characteristics of these orbits that are crucial to understanding observational phenomena such as quasi-periodic oscillations, which is a quite profound puzzle in the x-ray observational data of accretion disks (for a review, see for example [58–60]).

The paper's organization is as follows: q-metric is presented in Section II. The generalized q-metric is introduced in Section III, and the circular geodesic on the equatorial plane in the background of the generalized q-metric is discussed in Section IV. In Section V the circular geodesics in q-metric briefly revisited. Finally, a brief discussion presented in Section VI.

In this paper, the geometrized units where  $c = 1$  and  $G = 1$ , is used.

## II. q-METRIC

This particular space-time contains a quadrupole parameter, which is related to the compact object deformation. The metric represents the exterior gravitational field of an isolated static axisymmetric mass distribution and can be used to investigate the exterior fields of slightly deformed astrophysical objects in the strong-field regime [61, 62]. Thus the presence of quadrupole, independent of its value, changes the geometric properties of space-time drastically. The metric is presented as follows

$$ds^2 = \left(1 - \frac{2M}{r}\right)^{1+\alpha} dt^2 - \left(1 - \frac{2M}{r}\right)^{-\alpha} \left[ \left(1 + \frac{M^2 \sin^2 \theta}{r^2 - 2Mr}\right)^{-\alpha(2+\alpha)} \left( \frac{dr^2}{1 - \frac{2M}{r}} + r^2 d\theta^2 \right) + r^2 \sin^2 \theta d\phi^2 \right]. \quad (1)$$

However, in 1959, Erez and Rosen pointed out that the multipole structure of a static axially symmetric solution has a simpler form in the prolate spheroidal coordinates [63] rather than the cylindrical coordinates of Weyl [3, 11, 25]

$$ds^2 = - \left( \frac{x-1}{x+1} \right)^{(1+\alpha)} dt^2 + M^2 (x^2 - 1) \left( \frac{x+1}{x-1} \right)^{(1+\alpha)} \left[ \left( \frac{x^2 - 1}{x^2 - y^2} \right)^{\alpha(2+\alpha)} \left( \frac{dx^2}{x^2 - 1} + \frac{dy^2}{1 - y^2} \right) + (1 - y^2) d\phi^2 \right], \quad (2)$$

with the following transformation law

$$x = \frac{r}{M} - 1, \quad y = \cos \theta. \quad (3)$$

In fact, this metric has the central curvature singularity at  $x = -1$  where it is present for all real values of  $\alpha$ .

Moreover, an additional singularity appears at  $x = 1$ , which is also a horizon in the sense that the norm of the time-like Killing vector at this radius vanishes, and outside this hypersurface, there exists no additional horizon. However, considering relatively small quadrupole moment, this hypersurface is located very close to the origin of coordinates so that a physically reasonable interior solution could be used to cover them [61], and out of this region, there is no more singularity, and the metric outside a region that can be considered as the central deformed body is asymptotically flat. By Geroch definition [64], the lowest independent multipole moments for this metric is

$$m_0 = M(1 + \alpha), \quad (4)$$

where  $m_0$  is being positive to avoid having a negative mass distribution. It is equivalent to restricting quadrupole at most to this domain  $\alpha \in (-1, \infty)$  [65]. Of course, for  $\alpha = -1$  the flat space-time is recovered [24]. Also, the second multipole moment is calculated as [64],

$$m_2 = -\frac{M^3}{3}\alpha(1 + \alpha)(2 + \alpha), \quad (5)$$

where describes the deformation from the spherical case. It turns out that all higher multipole moments can be written in terms of  $m_0$  and  $m_2$  [61, 64]. This means, equivalently, the only independent parameters are  $M$  and  $\alpha$ , which determine the mass and quadrupole moment. Besides, all odd multipole moments vanish because of reflection symmetry concerning the equatorial plane.

### III. GENERALIZATION OF q-METRIC

The first static and axisymmetric solutions with arbitrary quadrupole moment are described by Weyl metric,

$$ds^2 = -e^{2\psi_0} dt^2 + e^{2(\gamma_0 - \psi_0)}(d\rho^2 + dz^2) + e^{-2\psi_0} \rho^2 d\phi^2, \quad (6)$$

where  $\psi = \psi(\rho, z)$  and  $\gamma = \gamma(\rho, z)$  are the metric functions. If we consider three-dimension manifold  $N$ , orthogonal to the static Killing vector field, then this metric induced the flat metric on  $N$ , and the metric function  $\psi$  plays the role of gravitational potential, and with respect to this flat metric, obeys the Laplace equation

$$\psi_{0,\rho\rho} + \frac{1}{\rho}\psi_{0,\rho} + \psi_{0,zz} = 0. \quad (7)$$

The field  $\psi$  satisfies Laplace's equation, while the field  $\gamma$  is determined by the relation [2]

$$\nabla\gamma_0\nabla\rho = \rho(\nabla\psi_0)^2, \quad (8)$$

where  $\nabla := \partial_\rho + i\partial_z$ , or

$$\begin{aligned} \gamma_{0,\rho} &= \rho(\psi_{0,\rho}^2 - \psi_{0,z}^2), \\ \gamma_{0,z} &= 2\rho\psi_{0,\rho}\psi_{0,z}. \end{aligned} \quad (9)$$

Now, the Weyl's technique takes advantage of the linearity of Laplace's equation for  $\psi$  and modifies our original metric by replacing the field  $\psi$  by

$$\psi = \psi_0 + \hat{\psi} \quad (10)$$

Since equation (8) is not linear with respect to  $\gamma_0$ , one can not, with the same modification, find a new field  $\hat{\gamma}$ . In fact, there will be also a contribution of  $\delta\gamma$  that satisfies

$$\nabla(\delta\gamma) = \mathcal{C}(\rho)(\nabla\psi_0), \quad (11)$$

where  $\mathcal{C}$  is a function of  $\rho$ . This relation determines  $\delta\gamma$  up to some constant. However, the requirement of elementary flatness [66], in the neighbourhood of the symmetry axis fixes the constant, and it should be set equal to zero.

To sum up, all the process reduces to choosing two fields that provide a solution of the vacuum field equations and take them as the seed for introducing new fields that satisfy above relations. In this approach, metric components are expressed through integrability conditions as functions of a single harmonic function and its partial derivatives in a surprisingly simple mathematical procedure.

Following Weyl's procedure by using the q-metric fields as a seed, we can obtain a solution of a deformed source with the existence of external mass distribution, which can be generalized to the whole class of q-metric. So, we introduce auxiliary fields  $\psi$  and  $\gamma$  such that

$$e^{2\psi} := \left(\frac{x-1}{x+1}\right)^{(1+\alpha)} e^{2\hat{\psi}}, \quad (12)$$

$$e^{2\gamma} := \left(\frac{x^2-1}{x^2-y^2}\right)^{\alpha(1+\alpha)} e^{2\hat{\gamma}}. \quad (13)$$

Notice that the exponential factor represents the surrounding matter, distorted terms. As this process suggests, we preserve the q-metric fields by taking  $\hat{\gamma} = \hat{\psi} = 0$ . It can easily be checked that in the limits  $\hat{\psi} = 0$ ,  $\hat{\gamma} = 0$ , and  $\alpha = 0$  we recover the Schwarzschild fields, and in the case  $\alpha = 0$ , but  $\hat{\gamma} \neq 0$ ,  $\hat{\psi} \neq 0$  we obtain the distorted Schwarzschild fields written in the prolate spheroidal coordinates.

In this way, field functions preserve their properties as before by its construction. The equations (7) and (9) in the prolate spheroidal coordinates are written as,

$$(x^2 - 1)\hat{\psi}_{,xx} + 2x\hat{\psi}_{,x} + \hat{\psi}_{,yy} + \frac{y}{\sqrt{1-y^2}}\hat{\psi}_{,y} = 0, \quad (14)$$

$$\hat{\gamma}_{,x} = \frac{y^2 - 1}{x^2 - y^2} \left[ x \left( \hat{\psi}_{,y}^2 - (x^2 - 1)\hat{\psi}_{,x}^2 \right) + \frac{2y(1-x^2)}{\sqrt{1-y^2}} \hat{\psi}_{,x} \hat{\psi}_{,y} \right], \quad (15)$$

$$\hat{\gamma}_{,y} = \frac{1-y^2}{x^2 - y^2} \left[ \frac{y}{\sqrt{1-y^2}} \left( \hat{\psi}_{,y}^2 - (x^2 - 1)\hat{\psi}_{,x}^2 \right) + 2x\hat{\psi}_{,y} \hat{\psi}_{,x} \right]. \quad (16)$$

Ultimately, the metric is then given by

$$ds^2 = - \left( \frac{x-1}{x+1} \right)^{(1+\alpha)} e^{2\hat{\psi}} dt^2 + M^2 (x^2 - 1) e^{-2\hat{\psi}} \left( \frac{x+1}{x-1} \right)^{(1+\alpha)} \left[ \left( \frac{x^2 - 1}{x^2 - y^2} \right)^{\alpha(2+\alpha)} e^{2\hat{\gamma}} \left( \frac{dx^2}{x^2 - 1} + \frac{dy^2}{1 - y^2} \right) + (1 - y^2) d\phi^2 \right], \quad (17)$$

where  $t \in (-\infty, +\infty)$ ,  $x \in (1, +\infty)$ ,  $y \in [-1, 1]$ , and  $\phi \in [0, 2\pi)$ . To see the explicit form of these functions, by the standard procedure via the separation of variables method in  $\psi$ , it generally can be expressed in terms of Legendre polynomials of the first kind and second kind [67]. This method was introduced first by Geroch and Hartle [9]. One can see the general form of these distortion functions is in terms of Legendre polynomial where, for example, in [10, equation 6-7]. However, up to the quadrupole  $\beta_2$ , these are expressed as follows [10],

$$\hat{\psi} = -\frac{\beta_2}{2} [-3x^2y^2 + x^2 + y^2 - 1], \quad (18)$$

$$\hat{\gamma} = -2x\beta_2(1-y^2) + \frac{\beta_2^2}{4}(x^2 - 1)(1-y^2)(-9x^2y^2 + x^2 + y^2 - 1). \quad (19)$$

For simplicity, in the rest of the paper, we refer to quadrupole in both cases without the index, namely  $\alpha$  and  $\beta$ . Also, we call  $\alpha$  deformation parameter and  $\beta$  distortion parameter in related works.

This metric contains three free parameters: the total mass, deformation parameter  $\alpha$ , and distortion  $\beta$ , which are taken to be relatively small and connected to the compact object deformation and external mass presence distribution, respectively. The result is also locally valid by its construction [7, 9], and may be considered also as the local q-metric or distorted q-metric. From the physics perspective, this solution is similar to the q-metric solution with an additional external gravitational field, similar to the addition of a magnetic environment to the black hole solution. [20–23].

In what follows, we explore the geodesic motion in this background.

#### IV. GEODESIC EQUATION

The geodesic equation in an arbitrary space-time is described by

$$\ddot{x}^\mu + \Gamma_{\nu\rho}^\mu \dot{x}^\nu \dot{x}^\rho = 0, \quad (20)$$

where derivatives are with respect to the affine parameter,  $\dot{x}^\mu$  is the four-velocity, and  $\Gamma_{\beta\gamma}^\alpha$  are the Christoffel symbols, which in this space-time read as follows

$$\Gamma_{tx}^t = \frac{(1+\alpha)}{x^2 - 1} + \hat{\psi}_{,x}, \quad (21)$$

$$\Gamma_{ty}^t = \hat{\psi}_{,y}, \quad (22)$$

$$\Gamma_{tt}^x = \frac{e^{4\hat{\psi}-2\hat{\gamma}}}{M^2} \left( \frac{x-1}{x+1} \right)^{2\alpha+1} \left( \frac{x^2 - y^2}{x^2 - 1} \right)^{\alpha(\alpha+2)} \left[ \frac{1+\alpha}{(x+1)^2} + \left( \frac{x-1}{x+1} \right) \hat{\psi}_{,x} \right], \quad (23)$$

$$\Gamma_{xx}^x = -\frac{1+\alpha}{x^2 - 1} + \frac{\alpha(\alpha+2)(y^2 - 1)(1+2x)}{(x^2 - 1)(x^2 - y^2)} + \hat{\gamma}_{,x} - \hat{\psi}_{,x}, \quad (24)$$

$$\Gamma_{xy}^x = -\frac{y\alpha(\alpha+2)}{x^2 - y^2} + \hat{\gamma}_{,y} - \hat{\psi}_{,y}, \quad (25)$$

$$\Gamma_{yy}^x = \left( \frac{1-x}{1-y^2} \right) \left[ 1 - \frac{\alpha}{x-1} + (\hat{\gamma}_{,x} - \hat{\psi}_{,x})(x+1) \right] - \frac{x}{(x^2 - y^2)} \alpha(\alpha+2), \quad (26)$$

$$\Gamma_{\phi\phi}^x = e^{-2\hat{\gamma}}(1-y^2) \left( \frac{x^2 - y^2}{x^2 - 1} \right)^{\alpha(\alpha+2)} \left[ 1 + \alpha - x + \hat{\psi}_{,x}(x^2 - 1) \right], \quad (27)$$

$$\Gamma_{tt}^y = \frac{e^{4\hat{\psi}-2\hat{\gamma}}}{M^2} \left( \frac{1-y^2}{x^2 - 1} \right) \left( \frac{x^2 - y^2}{x^2 - 1} \right)^{\alpha(\alpha+2)} \hat{\psi}_{,y}, \quad (28)$$

$$\Gamma_{xx}^y = \frac{y^2 - 1}{x^2 - 1} \left[ \frac{y\alpha(\alpha+2)}{x^2 - y^2} + \hat{\gamma}_{,y} - \hat{\psi}_{,y} \right], \quad (29)$$

$$\Gamma_{xy}^y = \frac{x-1-\alpha}{x^2 - 1} + \left( \frac{1-y^2}{x^2 - y^2} \right) x\alpha(2+\alpha) + \hat{\gamma}_{,x} - \hat{\psi}_{,x}, \quad (30)$$

$$\Gamma_{yy}^y = \frac{y}{1-y^2} + \frac{y\alpha(\alpha+2)}{x^2 - y^2} + \hat{\gamma}_{,y} - \hat{\psi}_{,y}, \quad (31)$$

$$\Gamma_{\phi\phi}^y = \left( \frac{x^2 - y^2}{x^2 - 1} \right)^{\alpha(2+\alpha)} (1-y^2) e^{-2\hat{\gamma}} \left[ y + \hat{\psi}_{,y}(1-y^2) \right], \quad (32)$$

$$\Gamma_{\phi x}^\phi = \frac{x-1-\alpha}{x^2 - 1} - \hat{\psi}_{,x}, \quad (33)$$

$$\Gamma_{\phi y}^\phi = \frac{y}{y^2 - 1} - \hat{\psi}_{,y}. \quad (34)$$

Regarding the symmetries in space-time, there are two constants of geodesic motion  $E$  and  $L$ ,

$$E = -g_{tt}\dot{t} = \left(\frac{x-1}{x+1}\right)^{(1+\alpha)} e^{2\hat{\psi}} \dot{t}, \quad (35)$$

$$L = g_{\phi\phi}\dot{\phi} = M^2(x^2-1) \left(\frac{x+1}{x-1}\right)^{(1+\alpha)} e^{-2\hat{\psi}} \dot{\phi}. \quad (36)$$

By using these relations and the normalization condition  $g_{\rho\nu}\dot{x}^\rho\dot{x}^\nu = -\epsilon$ , where  $\epsilon$  can take values  $-1$ ,  $0$  and  $1$ , for the space-like, light-like and for the time-like trajectories, respectively, then the geodesic equation (20) is reduced to

$$\left(1 + \frac{x^2-1}{x^2-y^2}\right)^{\alpha(2+\alpha)} M^2 e^{2\hat{\gamma}} \dot{x}^2 + V^2 = E^2, \quad (37)$$

where

$$V^2 = \frac{x^2-1}{1-y^2} \left(\frac{x^2-1}{x^2-y^2}\right)^{\alpha(2+\alpha)} M^2 e^{2\hat{\gamma}} \dot{y}^2 + \frac{L^2 e^{4\hat{\psi}}}{M^2(1-y^2)(x+1)^2} + \left(\frac{x-1}{x+1}\right)^{(\alpha+1)} e^{2\hat{\psi}} \epsilon. \quad (38)$$

One can interpret this equation as the motion along the  $x$  coordinate in terms of the so-called effective potential  $V^2$ . However, due to the appearance of  $\dot{y}$  in this expression, it is not a potential. In the next subsection, we rewrite  $V^2$  in the equatorial plane, so that it has the meaning of effective potential, and we rename it to  $V_{\text{Eff}}$  accordingly.

### A. Equatorial plane

In the equatorial plane  $y = 0$ , the distortion functions (18) up to the quadrupole simplify to

$$\hat{\psi} = -\frac{\beta}{2}(x^2-1), \quad (39)$$

$$\hat{\gamma} = -2\beta x + \frac{\beta^2}{4}(x^2-1)^2. \quad (40)$$

Also, due to reflection symmetry, we have the following condition for the existence of geodesics in the equatorial plane [62, 68]

$$\alpha_{2n-1} = 0 \text{ for } n > 0. \quad (41)$$

Then, the metric in the equatorial plane is given by

$$ds^2 = -\left(\frac{x-1}{x+1}\right)^{(1+\alpha)} e^{2\hat{\psi}} dt^2 + M^2(x^2-1) e^{-2\hat{\psi}} \left(\frac{x+1}{x-1}\right)^{(1+\alpha)} \left[ \left(\frac{x^2-1}{x^2}\right)^{\alpha(2+\alpha)} e^{2\hat{\gamma}} \left(\frac{dx^2}{x^2-1} + dy^2\right) + d\phi^2 \right]. \quad (42)$$

And the relation (37) is reduced to

$$\left(1 + \frac{x^2-1}{x^2}\right)^{\alpha(2+\alpha)} M^2 e^{2\hat{\gamma}} \dot{x}^2 + V_{\text{Eff}} = E^2, \quad (43)$$

where

$$V_{\text{Eff}} = \left(\frac{x-1}{x+1}\right)^{(\alpha+1)} e^{2\hat{\psi}} \left[ \epsilon + \frac{L^2 e^{2\hat{\psi}}}{M^2(x+1)^2} \left(\frac{x-1}{x+1}\right)^\alpha \right], \quad (44)$$

In the rest of this section, circular motion in the equatorial plane is studied.

### B. Circular orbits for the time-like trajectory

In this type of motion, there is no change in the  $x$  direction  $\dot{x} = 0$ , so one can study the motion of test particles in the effective potential (44) equivalently. Where  $V_{\text{Eff}}$  for  $\beta = 0$ , reduce to the effective potential for q-metric, and  $\alpha = 0$  corresponds to the effective potential for distorted Schwarzschild metric, and in the case of  $\alpha = \beta = 0$  the effective potential for Schwarzschild space-time.

In Figure 1,  $V_{\text{Eff}}$  is plotted for zero, positive and negative values of  $\alpha$  and  $\beta$ . As we see, the Schwarzschild effective potential lies in between the effective potential with a negative value of  $\alpha$  and the one with the positive value of  $\alpha$ . Also, for each fixed value of  $\alpha$ , the effective potential for a negative  $\beta$  is higher than the effective potential for the same  $\alpha$  but vanishing  $\beta$ . The opposite is also true for positive  $\beta$  at each  $x$ . As Figure 1 shows, further away from the central object, they are more diverged.

Typically, the place of ISCO, the last innermost stable orbit, is the place of the extrema of  $V_{\text{Eff}}$  and  $(V_{\text{Eff}})'$  simultaneously. However, finding extrema of  $V_{\text{Eff}}$ , equivalents to analysis the extrema of  $L^2$  for massive particle, and it is given by

$$L^2 = \frac{M^2(x+1)^{\alpha+2} [-\beta x^3 + \beta x + \alpha + 1]}{(x-1)^\alpha [2\beta x^3 + (1-2\beta)x - 2\alpha - 2]} e^{-2\hat{\psi}}. \quad (45)$$

The vertical asymptote of this function for  $x > 1$  is

$$2\beta x^3 + (1-2\beta)x - 2\alpha - 2 = 0, \quad (46)$$

which leads to this relation for  $\beta$

$$l_1 := \frac{-x + 2(\alpha + 1)}{2x(x^2 - 1)}. \quad (47)$$

In the space-time with the quadrupole (in general with multipole moments), there is an interesting possibility that there exists a curve in which  $L^2$  may vanish along



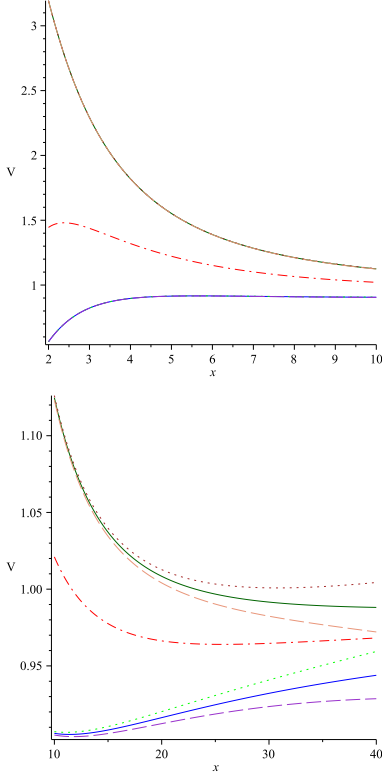


FIG. 1. Plots of  $V_{\text{EFF}}$  for different values of  $\alpha$  and  $\beta$ . In both plots, the dot-dashed line in the middle is Schwarzschild  $\alpha = \beta = 0$ , the solid line under the Schwarzschild corresponds to values  $(\alpha = 0.5, \beta = 0)$ , and the solid line above the Schwarzschild corresponds to  $(\alpha = -0.4, \beta = 0)$ . The dotted line under the Schwarzschild is for the values  $(\alpha = 0.5, \beta = -0.00001)$ , and the dotted line above the Schwarzschild is plotted for  $(\alpha = -0.4, \beta = -0.00001)$ . The dashed line under the Schwarzschild is for values  $(\alpha = 0.5, \beta = 0.00001)$ , and the dashed line above the Schwarzschild is plotted for  $(\alpha = -0.4, \beta = 0.00001)$ .

with it. This means that particles are at rest along this curve with respect to the central object. Of course, this is not the case in Schwarzschild space-time. In this way, the external matter manifests its existence by neutralizing the central object's gravitational effect at the region determined by this curve. In this case, this happens along  $-\beta x^3 + \beta x + \alpha + 1 = 0$ , which can be written also as

$$l_2 := \frac{\alpha + 1}{x(x^2 - 1)}. \quad (48)$$

However it is worth mentioning that, there is just one position for each chosen value of  $\beta$ . In general, the region between curves  $l_1$  (47) and  $l_2$  (48) defines the valid range for the distortion parameter  $\beta$ , due to the fact that  $L^2$  is a positive function. A straightforward calculation of  $\frac{d}{dx} L^2 = 0$  leads to

$$\begin{aligned} & 4x^3(x^2 - 1)^3\beta^3 \\ & + 6x^2(2x^2(2 - x^2)\alpha + x^5 - 2x^4 + 4x^2 + x - 2)\beta^2 \\ & + 4x(3x(x^2 - 1)\alpha^2 + 3x(-x^3 + 2x^2 + x - 3)\alpha \\ & + x^5 - 3x^4 + 8x^3 + 3x^2 - 3x)\beta \\ & - (\alpha + 1)x^2 + 6(\alpha + 1)^2x - 4\alpha^3 - 12\alpha^2 - 13\alpha - 5 \\ & = 0. \end{aligned} \quad (49)$$

Which gives the solution for  $\beta$  as

$$\beta = \frac{1}{2x(x^2 - 1)} \left( \frac{\sqrt[3]{D^2} - 3x^2}{3\sqrt[3]{D}} + 2 - x + 2\alpha \right), \quad (50)$$

where

$$D = 27x^3 - 81x^2(\alpha + 1) + 27(\alpha + 1) + 3\sqrt{\Delta}, \quad (51)$$

and

$$\begin{aligned} \Delta &= 84x^6 - 486x^5(\alpha + 1) + 729x^4(\alpha + 1)^2 \\ &+ 162x^3(\alpha + 1) - 486x^2(\alpha + 1)^2 + 81(\alpha + 1)^3. \end{aligned} \quad (52)$$

An analyze shows that for any value of  $\alpha$  chosen in this domain  $[-0.5, \infty)$ , the minimum of  $\beta$  is obtained at the intersection of the curve  $\beta$  (50) with  $l_1$  (47). Besides, the maximum of the curve  $\beta$  in the valid region is determined by the maximum of  $\beta$  for this chosen  $\alpha$ . For instance, in Figure 2, 3 and 4,  $\beta$  and the valid region for  $\alpha = 1$ ,  $\alpha = -0.4$ , and  $\alpha = -0.5$  is plotted. In the later, the minimum of  $\beta$  is obtained by its intersection with  $l_1$  (47), placed at the very close to outer singularity.

For the values of  $\alpha$  in this domain  $[-1 + \frac{\sqrt{5}}{5}, -0.5]$ , the curve  $\beta$  behaves differently, and it always lies in the valid region, so the minimum and maximum of  $\beta$  are determined by its extrema. In the plot 5, the minimum for  $\alpha = -0.526$  was shown, which its minimum is obtained by the minimum of a curve  $\beta$  itself.

It turns out that the maximum value of  $\beta$  is a monotonically decreasing function of  $\alpha$ . However, the place of ISCO for a maximum of  $\beta$  is a monotonically increasing function of  $\alpha$ . In addition, the minimum of  $\beta$  is an decreasing function of  $\alpha$  from  $\alpha = -1 + \frac{\sqrt{5}}{5}$  to  $\alpha = -0.5$ , and from this value it is monotonically increases. Also, we have the same pattern for ISCO for the minimum of  $\beta$ , see Figure 6.

To summarize, the minimum of  $\beta$  is obtained in the case  $\alpha = -0.5$ , and the maximum of  $\beta$  is reached for  $\alpha = -1 + \frac{\sqrt{5}}{5}$ . In Table VII, the values of minimum and maximum of  $\beta$  for various chosen values of  $\alpha$  are presented. Besides, the places of ISCO in the cases of maximum, minimum, and vanishing external quadrupole distortion parameter  $\beta$  are shown. We have seen for  $\alpha = \beta = 0$ , the place of ISCO for Schwarzschild is recovered at  $x = 5$ , and for  $\alpha = 0$ , ISCO in the case of

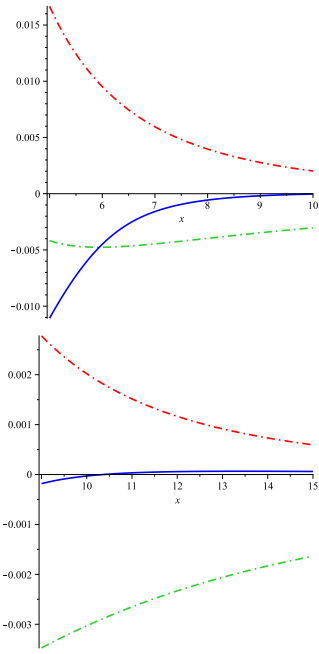


FIG. 2. The dashed lines are  $l_1$  (47) and  $l_2$  (48). The solid lines are the plots of  $\beta$  (50) for  $\alpha = 1$ , noted as  $\beta^{\alpha=1}$ . Minimum of  $\beta^{\alpha=1}$  is  $-0.0047632$  at  $x = 5.94338$ , and maximum of  $\beta^{\alpha=1}$  is  $0.0000659$  at  $x = 13.38972$ . Also,  $\beta = 0$  at  $x = 10.35890$ , so this  $x$  shows the value of ISCO for  $\alpha = 1$  without any external quadrupole  $\beta = 0$ .

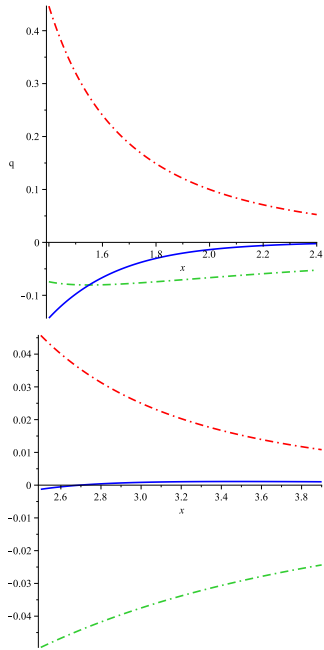


FIG. 3. The dashed lines are  $l_1$  (47) and  $l_2$  (48). The solid lines are plots of  $\beta$  (50) for  $\alpha = -0.4$ , noted as  $\beta^{\alpha=-0.4}$ . Minimum of  $\beta^{\alpha=-0.4}$  is  $-0.0805014$  at  $x = 1.55038$ , and maximum of  $\beta^{\alpha=-0.4}$  is  $0.0011090$  at  $x = 3.47165$ . Also,  $\beta = 0$  at  $x = 2.69443$ , so this  $x$  shows the value of ISCO for  $\alpha = -0.4$  without any external quadrupole  $\beta = 0$ .

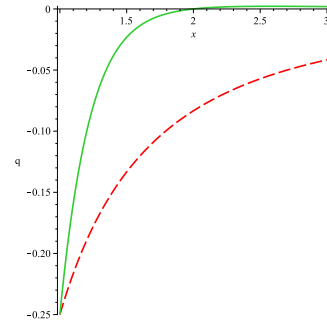


FIG. 4. At this value  $\alpha = -0.5$  curve  $\beta$  begins to intersect with curve 1 (47). Before this value, the minimum is determined by the minimum of  $\beta$  itself, and after that, the minimum of  $\beta$  is obtained by the intersection of these two curves.

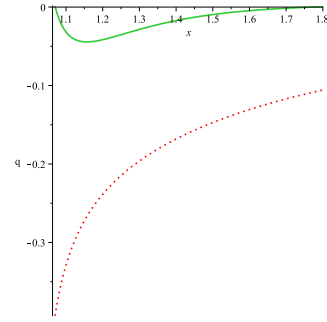


FIG. 5. Dotted line is  $l_1$  (47), and solid line is  $\beta$  (50) for  $\alpha = -0.526$ . In this interval  $[-1 + \frac{\sqrt{5}}{5}, -0.5)$  the minimum is determined by the minimum of the curve  $\beta$  (50) itself.

distorted Schwarzschild for different values of  $\beta$  have presented. However, we should mention that  $\beta$  is a parameter chosen for the entire space-time. It is not that  $\beta$  is not allowed to have certain values outside the specified bounds; when  $\beta$  is outside of the bounds, there will be no circular orbits at the given  $x$  (similar to  $r < 3M$  in Schwarzschild space-time).

### C. Circular orbits for the light-like trajectory

In this case,  $\epsilon = 0$ , and the effective potential (44) for light-like geodesics is reduced to

$$V_{\text{Eff}} = \left( \frac{x-1}{x+1} \right)^{(\alpha+1)} e^{2\hat{\psi}} \left[ \frac{L^2 e^{2\hat{\psi}}}{M^2 (x+1)^2} \left( \frac{x-1}{x+1} \right)^\alpha \right]. \quad (53)$$

In fact, a straightforward analysis of the effective potential shows that its first derivative vanishes for

$$\alpha = \frac{1}{2}(2\beta x^3 - 2\beta x + x - 2), \quad (54)$$

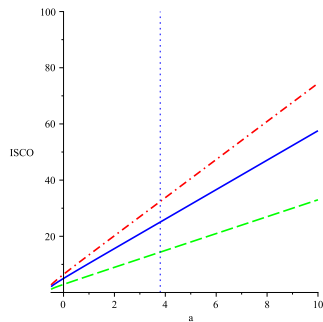


FIG. 6. The solid line is ISCO for  $\beta = 0$ , the dot-dashed line is ISCO for  $\beta_{\max}$ , and the dashed line is ISCO for  $\beta_{\min}$ . In all cases, ISCO is a monotonically increasing function of  $\alpha$ . Also, any vertical line, meaning  $\alpha = \text{constant}$ , intersects with all lines. This shows the place of ISCO at a fixed  $\alpha$  for a negative value of  $\beta$ ,  $\beta = 0$  and a positive value of  $\beta$ , simultaneously. So, the ISCO is also a monotonically increasing function of  $\beta$ .

where for  $\alpha = \beta = 0$ , it reduces to the Schwarzschild value  $x = 2$  equivalently to  $r = 3M$  in the standard Schwarzschild coordinates (3). Furthermore, the relation (54) is the limiting curve for time-like circular geodesics, curve  $l_1$  (47), which is written in terms of  $\alpha$ .

By inserting the relation (54) for  $\alpha$ , into the second derivative of the effective potential  $(V_{\text{eff}})''$ , we obtain a very interesting result. The second derivative vanishes along

$$\beta = -\frac{1}{2(3x^2 - 1)}. \quad (55)$$

This expression is also the minimum of the curve (54). Surprisingly, this means that for some negative values of  $\beta$  we have a bound photon orbit in the equatorial plane in this space-time, which is not the case nor in Schwarzschild spacetime, neither in  $q$ -metric. In fact, this arises due to the existence of quadrupole related to the external source. From this relation (55) one can find the places of ISCO and the negative values for quadrupole, which lead to having ISCO for light-like geodesics

$$\beta \in \left(-\frac{1}{4}, 0\right). \quad (56)$$

There is no surprise that the minimum value of  $\beta$  in the case of light-like trajectories coincides with the minimum value of  $\beta$  in the case of time-like trajectories, which occurs for the choice of  $\alpha = -0.5$ , see Table VII.

## V. REVISIT CIRCULAR GEODESICS IN $q$ -METRIC

In this section, following the discussion to have a comparison with the other case, we briefly revisit circular

motion on the equatorial plane in the  $q$ -metric with this slightly different approach from the studies in the literature, for example [24–26].

### A. Time-like geodesics in $q$ -metric

In this case, the specific angular momentum (45) is reduced to

$$L^2 = \frac{M^2(x+1)^{\alpha+2}(1+\alpha)}{(x-1)^\alpha[x-2(1+\alpha)]}. \quad (57)$$

An analyzing of  $\frac{d}{dx}L^2$ , like the previous case, shows the vertical asymptote to this function for  $x > 1$  is

$$k_1 := \frac{x}{2} - 1. \quad (58)$$

Also,  $L^2$  vanishes along this curve

$$k_2 := -1. \quad (59)$$

This value is the infimum value for  $\alpha$ , since regarding the domain of  $\alpha = (-1, \infty)$ , for  $\alpha = -1$  we obtain  $m_0 = 0$  in (4), also all other multipole moments vanish and the space-time will be flat as mentioned before. The region between curves  $k_1$  (58) and  $k_2$  (59), defines the valid range for  $\alpha$ , considering  $L^2$  is a positive function. A direct calculation for the extrema of  $L^2$ , leads to

$$\alpha_{\pm} = \frac{3}{4}x - 1 \pm \frac{1}{4}\sqrt{5x^2 - 4}. \quad (60)$$

This equation is polynomial rank two, unlike the previous case, and we can analyze it in the following way. Since for the domain of our interest  $x > 1$ , this relation  $5x^2 - 4 > 0$  satisfies, therefore we always have two curves  $\alpha_-$  and  $\alpha_+$ . In fact,  $\alpha_+$  lies out of the valid region between  $\alpha_1$  and  $\alpha_2$ , for all  $x > 1$ . However,  $\alpha_-$  intersect with  $\alpha_1$  and enter to the region at  $x = 1$ , where  $\alpha_-(1) = -\frac{1}{2}$ , and always remain inside this region (see Figure 7).

One can show that  $\alpha_-$  has a minimum inside this region at  $x = 3\frac{\sqrt{5}}{5} \approx 1.3416$ , where  $\alpha_-^{\min} = -1 + \frac{\sqrt{5}}{5} \approx -0.55279$ , and after this point,  $\alpha_-$  is a monotonically increasing function. So in this case, the domain of  $\alpha$  is  $[-1 + \frac{\sqrt{5}}{5}, \infty)$ .

For obtaining ISCOs, we rewrite equation  $L^2_{,x} = 0$ , in terms of  $x$ ,

$$x_{\pm} = 3 + 3\alpha \pm \sqrt{\Delta}, \quad \Delta = 5\alpha^2 + 10\alpha + 4. \quad (61)$$

By using the above analysis for  $\alpha_{\pm}$ , and rewrite (58) and (59) in terms of  $x$ , we obtain



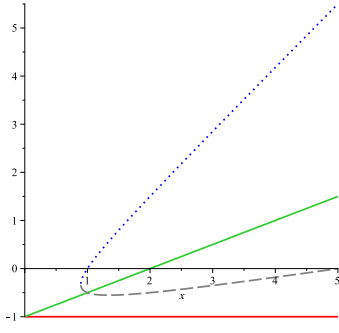


FIG. 7. Solid lines  $\alpha_2$  and  $\alpha_1$  show the valid region, where dashed line  $\alpha_-$  always lies in this region and dotted line  $\alpha_+$  is out of this region for any choice of  $\alpha$ .

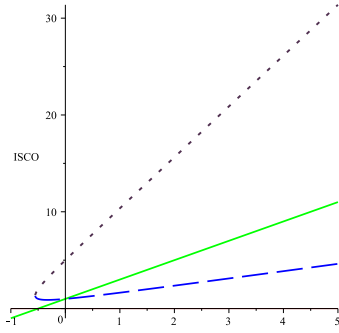


FIG. 8. Solid lines  $x_1 = 2\alpha + 1$  and  $x_2 = 0$ , show the valid region, where the dashed line  $x_+$  always lies in this region and dots line  $x_-$  is outside, for any choice of  $\alpha$ .

$$x_1 = 2\alpha + 1, \quad (62)$$

$$x_2 = 0. \quad (63)$$

If we plot them with  $x_+$  and  $x_-$  (61) together, we see that the corresponding valid ISCOs are obtained by  $x_+ (= x_{\text{ISCO}})$  (see Figure 8). Furthermore, this relation (61) shows that  $\Delta \geq 0$  is equivalent to  $\alpha$  be in this interval  $[-\infty, -1 - \frac{\sqrt{5}}{5}] \cup [-1 + \frac{\sqrt{5}}{5}, +\infty)$ , where only the second part, meaning  $[-1 + \frac{\sqrt{5}}{5}, \infty)$ , lies in the valid region. Consequently, this gives us no new information on the domain of  $\alpha$  more than what we have obtained before.

Again, we can see how ISCOs positions evolve as  $\alpha$  increases by plotting  $x_+ (= x_{\text{ISCO}})$ . the place of ISCO in Schwarzschild is at  $x = 5$  (equivalent to  $r = 6M$ ). For a negative  $\alpha$ , ISCO is closer to the horizon  $x = 1$ , and for a positive  $\alpha$  the place of ISCO is going farther, see Figure 9.

### B. Light-like geodesics for q-metric

In this case, the effective potential (53) is reduced to

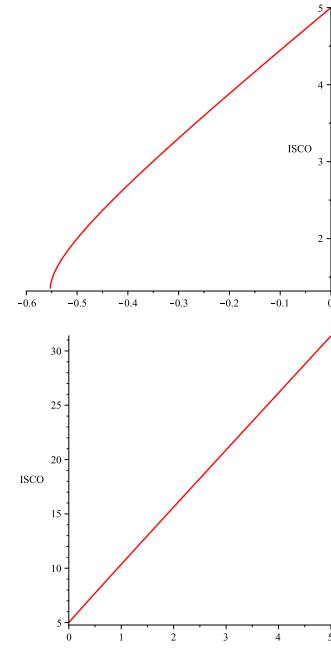


FIG. 9. Evolution of ISCO with  $\alpha$ , where the domain of  $\alpha$  is  $[-0.5528, +\infty)$ . The value of ISCO at  $\alpha = -0.5528$  is 1.3416. The place of ISCO for  $\alpha < 0$  is below the Schwarzschild value  $x = 5$  and for  $\alpha > 0$  is upper.

$$V_{\text{Eff}} = \left( \frac{x-1}{x+1} \right)^{(\alpha+1)} \left[ \frac{L^2}{M^2(x+1)^2} \left( \frac{x-1}{x+1} \right)^\alpha \right], \quad (64)$$

and the straightforward calculation shows that its first derivative vanishes along

$$x = 2 + 2\alpha. \quad (65)$$

So for any chosen value of  $\alpha$ , one obtains a value for  $x$ . Of course, in the case of  $\alpha = 0$ , Schwarzschild metric, we obtain  $x = 2$  or equivalently  $r = 3M$  with the transformation law (3). Moreover, the sign of the second derivative of the effective potential for this value of  $x$ , and any chosen value for  $\alpha$ , is negative, unlike the previous case indicating this circular motion is unstable.

## VI. SUMMARY AND CONCLUSION

This paper has presented a generalized q-metric for the relatively small quadrupole moment via Weyl's procedure. This metric explains the exterior of a deformed body locally in the presence of an external distribution of matter up to the quadrupole. It contains three free parameters: the total mass, deformation parameter  $\alpha$ , and the distortion parameter  $\beta$ , referring to the central object's quadrupoles and its surrounding mass distribution.

TABLE I. The minimum and the maximum of  $\beta$  and the place of ISCO for different values of  $\alpha$ . The letter  $\alpha$  appearing as the upper index in  $\beta$  and  $x$  means it is calculated concerning a fixed value of  $\alpha$

$\alpha$	$\beta_{\min}^{\alpha}$	$x_{\beta-\min}^{\alpha}$	$\beta_{\max}^{\alpha}$	$x_{\beta-\max}^{\alpha}$	$x_{\beta=0}^{\alpha}$
-0.5528	-0.0006262	1.333070	0.0040976	1.93984	1.40333
-0.526	-0.0443754	1.15685	0.0028270	2.30093	1.77325
-0.5	-0.2499996	1.000001	0.00217281	2.58141	2.00000
-0.49	-0.1757730	1.13203	0.0019932	2.68029	2.07818
-0.4	-0.0805014	1.55038	0.0011090	3.47165	2.69443
0	-0.0209443	2.87940	0.0002927	6.45602	5.00000
0.5	-0.0086651	4.42340	0.0001202	9.95281	7.70156
1	-0.0047632	5.94338	0.0000659	13.38972	10.35890
10	-0.0001533	32.98501	0.0000021	74.44744	57.57641

One can interpret it to represent a static, axisymmetric compact object in the presence of an external distribution of matter. This is valid for arbitrary deformation parameter  $\alpha > -1$ . However, these two parameters,  $\alpha$  and  $\beta$ , are not independent of each other.

Exercising the quadrupole moments may open an opportunity to consider them as new degrees of freedom to both central object and its surrounding, to search for their observational fingerprints, for instance, in the study of the gravitational wave, or quasi-periodic oscillations generated by a non-isolated, self-gravitating axisymmetric distribution of mass.

We propose that this class has promising features, and it may serve to link the metric to the physical nature of the compact object via its parameters. Although, as explained before, the  $q$ -metric metric is singular, to begin with, still this generalization worth considering to have more vacuum metric available, for example, to study a vacuum solution that is accelerating or embedded in an external field. Therefore, it may be of some interest to investigate how the external field affects the geometry and geodesics of the  $q$ -metric.

Furthermore, we carried out a characterization of quadrupole parameters' impact via studying the circular geodesics on the equatorial plane. Also, we have shown the valid ranges of distortion parameter  $\beta$ , for each choice of deformation parameter  $\alpha$ , for time-like and light-like trajectories. Some of the examples are listed in Table VII. In consequence, we found out for each choice of  $\alpha$  there are ISCOs for time-like geodesics for  $\beta \in [\beta_{\min}^{\alpha}, \beta_{\max}^{\alpha}]$  such that in general  $\beta_{\min} \approx -2.5 \times 10^{-1}$  at  $\alpha = -0.5$  and

$\beta_{\max} \approx 4.1 \times 10^{-3}$  at  $\alpha = -0.5528$ . Besides, in general, the place of ISCO is closer to the horizon for negative quadrupole moments; however, in the case of positive quadrupole moments, it is farther away, see Figure 6.

An interesting result is that there is a bound orbit for light-like geodesics on the equatorial plane, neither in Schwarzschild nor in  $q$ -metric. The key point is this bound orbit's existence relies on having the negative quadrupole of external matter and provides the valid range for  $\beta \in (-0.25, 0)$  in this case. In fact, most of our information about the astrophysical environment is obtained from electromagnetic radiation and consequently by studying the null geodesics; therefore, this result is of great astrophysical interest. Additionally, as an example of this applied procedure, we discussed circular geodesics on the equatorial plane of  $q$ -metric and the places of ISCO as a special case.

The next step of this work could be a study on off-equatorial time-like and light-like geodesics. Studying the topological implication of this background may be the next stage of study in this area. Also, the construction of accretion disks, the study of gravitational waves and quasi-periodic oscillation in this background are in the progress.

## VII. ACKNOWLEDGEMENTS

The author gratefully acknowledges Prof. Hernando Quevedo and Dr. Eva Hackmann for their valuable comments on this work. Thanks to the research training group GRK 1620, "Models of Gravity," funded by the German Research Foundation (DFG).

- 
- [1] Hans Stephani, Dietrich Kramer, Malcolm MacCallum, Cornelius Hoenselaers, and Eduard Herlt. *Exact solutions of Einstein's field equations*. 2003.
  - [2] Hermann Weyl. Zur gravitationstheorie. *Annalen der Physik*, 359(18):117–145, 1917.
  - [3] G. Erez and N. Rosen. The gravitational field of a particle possessing a multipole moment. *Bull. Research Council*

*Israel*, Vol: Sect. F.8, 9 1959.

- [4] David M. Zipoy. Topology of some spheroidal metrics. *Journal of Mathematical Physics*, 7(6):1137–1143, 1966.
- [5] B. H. Voorhees. Static axially symmetric gravitational fields. *Phys. Rev. D*, 2:2119–2122, Nov 1970.
- [6] Hernando Quevedo. Mass Quadrupole as a Source of Naked Singularities. *International Journal of Modern*

- Physics D*, 20(10):1779–1787, January 2011.
- [7] S Chandrasekhar. *The mathematical theory of black holes*. Oxford classic texts in the physical sciences. Oxford Univ. Press, Oxford, 2002.
  - [8] A. G. Doroshkevich, Y. B. Zel’dovich, and I. D. Novikov. Gravitational Collapse of Non-Symmetric and Rotating Bodies. *Zhurnal Eksperimentalnoi i Teoreticheskoi Fiziki*, 4:170, December 1965.
  - [9] R. Geroch and J. B. Hartle. Distorted black holes. *Journal of Mathematical Physics*, 23:680–692, 1982.
  - [10] Nora Bretón, Tatiana E. Denisova, and Vladimir S. Manko. A Kerr black hole in the external gravitational field. *Physics Letters A*, 230:7–11, Feb 1997.
  - [11] Hernando Quevedo. General static axisymmetric solution of einstein’s vacuum field equations in prolate spheroidal coordinates. *Phys. Rev. D*, 39:2904–2911, May 1989.
  - [12] V S Manko. On the description of the external field of a static deformed mass. *Classical and Quantum Gravity*, 7(9):L209–L211, sep 1990.
  - [13] J Castejon-Amenedo and V S Manko. On a stationary rotating mass with an arbitrary multipole structure. *Classical and Quantum Gravity*, 7(5):779–785, may 1990.
  - [14] Norman Gürlebeck. Source integrals for multipole moments in static and axially symmetric spacetimes. *Phys. Rev. D*, 90:024041, Jul 2014.
  - [15] S. Toktarbay and H. Quevedo. A stationary q-metric. *Gravitation and Cosmology*, 20(4):252–254, Oct 2014.
  - [16] H. Quevedo. Multipole moments in general relativity—static and stationary vacuum solutions—. *Fortschritte der Physik/Progress of Physics*, 38(10):733–840, 1990.
  - [17] Hernando Quevedo and Bahram Mashhoon. Exterior gravitational field of a rotating deformed mass. *Physics Letters A*, 109(1):13 – 18, 1985.
  - [18] Wai-Mo Suen. Distorted black holes in terms of multipole moments. *Phys. Rev. D*, 34:3633–3637, Dec 1986.
  - [19] N. Bretón, A. A. García, V. S. Manko, and T. E. Denisova. Arbitrarily deformed kerr-newman black hole in an external gravitational field. *Phys. Rev. D*, 57:3382–3388, Mar 1998.
  - [20] F. J. Ernst. Black holes in a magnetic universe. *Journal of Mathematical Physics*, 17(1):54–56, January 1976.
  - [21] Frederick J. Ernst and Walter J. Wild. Kerr black holes in a magnetic universe. *Journal of Mathematical Physics*, 17(2):182–184, February 1976.
  - [22] Robert M. Wald. Black hole in a uniform magnetic field. *Phys. Rev. D*, 10:1680–1685, Sep 1974.
  - [23] Mustapha Azreg-Aïnou. Vacuum and nonvacuum black holes in a uniform magnetic field. *European Physical Journal C*, 76(7):414, July 2016.
  - [24] K. Boshkayev, E. Gasperín, A. C. Gutiérrez-Piñeres, H. Quevedo, and S. Toktarbay. Motion of test particles in the field of a naked singularity. *Phys. Rev. D*, 93:024024, Jan 2016.
  - [25] Hernando Quevedo. Mass quadrupole as a source of naked singularities. *International Journal of Modern Physics D*, 20(10):1779–1787, 2011.
  - [26] K. A. Boshkayev, H. Quevedo, M. S. Abutalip, Zh. A. Kalyanova, and Sh. S. Suleymanova. Geodesics in the field of a rotating deformed gravitational source. *International Journal of Modern Physics A*, 31(02n03):1641006, 2016.
  - [27] Georgios Lukes-Gerakopoulos. Nonintegrability of the Zipoy-Voorhees metric. *Phys. Rev. D*, 86(4):044013, August 2012.
  - [28] Demetrios Papadopoulos, Bob Stewart, and Louis Witten. Some properties of a particular static, axially symmetric space-time. *Phys. Rev. D*, 24:320–326, Jul 1981.
  - [29] S. L. Parnovskii. The type and structure of time-like singularities in the general theory of relativity - From the gamma-metric to a general solution. *Zhurnal Eksperimentalnoi i Teoreticheskoi Fiziki*, 88:1921–1937, June 1985.
  - [30] L. Herrera, G. Magli, and D. Malafarina. Non-spherical sources of static gravitational fields: Investigating the boundaries of the no-hair theorem. *General Relativity and Gravitation*, 37(8):1371–1383, August 2005.
  - [31] Hideo Kodama and Wataru Hikida. Global structure of the Zipoy Voorhees Weyl spacetime and the dgr = 2 Tomimatsu Sato spacetime. *Classical and Quantum Gravity*, 20(23):5121–5140, December 2003.
  - [32] Gary W. Gibbons and Mikhail S. Volkov. Weyl metrics and wormholes. *J. Cosmol. Astropart. Phys*, 2017(5):039, May 2017.
  - [33] Anirban N. Chowdhury, Mandar Patil, Daniele Malafarina, and Pankaj S. Joshi. Circular geodesics and accretion disks in the janis-newman-winicour and gamma metric spacetimes. *Phys. Rev. D*, 85:104031, May 2012.
  - [34] K. Boshkayev, E. Gasperín, A. C. Gutiérrez-Piñeres, H. Quevedo, and S. Toktarbay. Motion of test particles in the field of a naked singularity. *Phys. Rev. D*, 93(2):024024, January 2016.
  - [35] V. P. Neznamov and V. E. Shemarulin. Motion of spin-half particles in the axially symmetric field of naked singularities of the static q-metric. *Gravitation and Cosmology*, 23(2):149–161, April 2017.
  - [36] Bobir Toshmatov, Daniele Malafarina, and Naresh Dadhich. Harmonic oscillations of neutral particles in the  $\gamma$  metric. *Phys. Rev. D*, 100:044001, Aug 2019.
  - [37] Abraão J. S. Capistrano, Paola T. Z. Seidel, and Luís A. Cabral. Effective apsidal precession from a monopole solution in a Zipoy spacetime. *European Physical Journal C*, 79(9):730, September 2019.
  - [38] José P. S. Lemos and Oleg B. Zaslavskii. Black hole mimickers: Regular versus singular behavior. *Phys. Rev. D*, 78:024040, Jul 2008.
  - [39] Rajibul Shaikh, Prashant Kocherlakota, Ramesh Narayan, and Pankaj S. Joshi. Shadows of spherically symmetric black holes and naked singularities. *MNRAS*, 482(1):52–64, January 2019.
  - [40] M. A. Abramowicz, W. Kluźniak, and J. P. Lasota. No observational proof of the black-hole event-horizon. *Astron Astroph*, 396:L31–L34, December 2002.
  - [41] Fintan D. Ryan. Gravitational waves from the inspiral of a compact object into a massive, axisymmetric body with arbitrary multipole moments. *Phys. Rev. D*, 52(10):5707–5718, November 1995.
  - [42] Chao Li and Geoffrey Lovelace. Generalization of Ryan’s theorem: Probing tidal coupling with gravitational waves from nearly circular, nearly equatorial, extreme-mass-ratio inspirals. *Phys. Rev. D*, 77(6):064022, March 2008.
  - [43] George Pappas and Theocharis A. Apostolatos. Revising the multipole moments of numerical spacetimes and its consequences. *Phys. Rev. Lett.*, 108:231104, Jun 2012.
  - [44] Sayak Datta and Sukanta Bose. Probing the nature of central objects in extreme-mass-ratio inspirals with gravitational waves. *Phys. Rev. D*, 99(8):084001, April 2019.
  - [45] J. Horský. A comment of thin shells in general relativity. *Physics Letters A*, 28(9):599–599, February 1969.

- [46] M. Bursa, M. A. Abramowicz, V. Karas, and W. Kluźniak. The Upper Kilohertz Quasi-periodic Oscillation: A Gravitationally Lensed Vertical Oscillation. *Astrophys. J*, 617(1):L45–L48, December 2004.
- [47] Andrey A. Shoom, Cole Walsh, and Ivan Booth. Geodesic motion around a distorted static black hole. *Physical Review D*, 93(6), Mar 2016.
- [48] Jutta Kunz, Petya Nedkova, and Stoytcho Yazadjiev. Magnetized black holes in an external gravitational field. *Phys. Rev. D*, 96:024017, Jul 2017.
- [49] Patricio S. Letelier. Stability of circular orbits of particles moving around black holes surrounded by axially symmetric structures. *Phys. Rev. D*, 68:104002, Nov 2003.
- [50] Javier Ramos-Caro, Juan F. Pedraza, and Patricio S. Letelier. Motion around a monopole + ring system – i. stability of equatorial circular orbits versus regularity of three-dimensional motion. *Monthly Notices of the Royal Astronomical Society*, 414(4):3105–3116, 2011.
- [51] Bruno Boisseau and Patricio S. Letelier. Relativistic multipoles and the advance of the perihelia. *General Relativity and Gravitation*, 34(7):1077–1096, Jul 2002.
- [52] Framsol López-Suspes and Guillermo A. González. Equatorial circular orbits of neutral test particles in weyl spacetimes. *Brazilian Journal of Physics*, 44(4):385–397, Aug 2014.
- [53] O. Semerák. Circular orbits in stationary axisymmetric spacetimes. *General Relativity and Gravitation*, 30(8):1203–1215, Aug 1998.
- [54] Patricio S Letelier. On the gravitational field of static and stationary axial symmetric bodies with multi-polar structure. *Classical and Quantum Gravity*, 16(4):1207–1213, jan 1999.
- [55] Eduardo Guéron and Patricio S. Letelier. Chaotic motion around prolate deformed bodies. *Phys. Rev. E*, 63:035201, Feb 2001.
- [56] Eduardo Guéron and Patricio S. Letelier. Geodesic chaos around quadrupolar deformed centers of attraction. *Phys. Rev. E*, 66:046611, Oct 2002.
- [57] M. Žáček and Oldrich Semerak. Gravitating discs around a schwarzschild black hole ii. *Czechoslovak Journal of Physics*, 52:19–27, 01 2002.
- [58] M. van der Klis. Millisecond Oscillations in X-ray Binaries. *Annual Review of Astronomy and Astrophysics*, 38:717–760, January 2000.
- [59] Jeffrey E. McClintock and Ronald A. Remillard. *Black hole binaries*, volume 39, pages 157–213. Oxford, 2006.
- [60] Adam Ingram and Sara Motta. A review of quasi-periodic oscillations from black hole X-ray binaries: observation and theory. *arXiv e-prints*, page arXiv:2001.08758, January 2020.
- [61] Hernando Quevedo. Exterior and interior metrics with quadrupole moment. *Gen. Rel. Grav.*, 43:1141–1152, 2011.
- [62] K. Boshkayev, E. Gasperin, A. C. Gutierrez-Pineros, H. Quevedo, and S. Toktarbay. Motion of test particles in the field of a naked singularity. *Phys. Rev.*, D93(2):024024, 2016.
- [63] Prolate spheroidal coordinates are three-dimensional orthogonal coordinates that result from rotating the two-dimensional elliptic coordinates about the focal axis of the ellipse.
- [64] R. Geroch. Multipole Moments. II. Curved Space. *Journal of Mathematical Physics*, 11:2580–2588, August 1970.
- [65] In fact, the Arnowitt-Deser-Misner mass which characterizes the physical properties of the exact solution also has the same expression and should be positive [24, App.], also for stationary space-time it is equivalent to Komar mass.
- [66] In general, both functions  $\gamma$  and  $\psi$  should be regular at the symmetry axis  $y = \pm 1$  [10]. Sometimes this condition is referred to as the elementary flatness condition.
- [67] Milton Abramowitz. *Handbook of Mathematical Functions, With Formulas, Graphs, and Mathematical Tables*,. Dover Publications, Inc., New York, NY, USA, 1974.
- [68] Nora Bretón, Tatiana E. Denisova, and Vladimir S. Manko. A kerr black hole in the external gravitational field. *Physics Letters A*, 230(1):7 – 11, 1997.